

Corneal Application of R9-SOCS1-KIR Peptide Alleviates Endotoxin-Induced Uveitis

Chulbul M. Ahmed¹, Anil P. Patel¹, Cristhian J. Ildefonso², Howard M. Johnson³, and Alfred S. Lewin¹

¹ Department of Molecular Genetics and Microbiology, University of Florida, Gainesville, Florida, USA

² Department of Ophthalmology, University of Florida, Gainesville, Florida, USA

³ Department of Microbiology and Cell Science, University of Florida, Gainesville, Florida, USA

Correspondence: Alfred S. Lewin, Department of Molecular Genetics and Microbiology, University of Florida, Gainesville, FL 32610, Florida, USA.

e-mail: lewin@ufl.edu

Received: August 6, 2020

Accepted: February 9, 2021

Published: March 24, 2021

Keywords: uveitis; mouse model; lipopolysaccharide; immune suppression; peptide delivery

Citation: Ahmed CM, Patel AP, Ildefonso CJ, Johnson HM, Lewin AS. Corneal application of R9-SOCS1-KIR peptide alleviates endotoxin-induced uveitis. *Trans Vis Sci Tech.* 2021;10(3):25, <https://doi.org/10.1167/tvst.10.3.25>

Purpose: Uveitis is an ocular inflammation that can affect individuals of all ages and is a major cause of blindness. We have tested the therapeutic efficacy of a cell penetrating peptide from the kinase inhibitory region of suppressor of cytokine signaling 1, denoted as R9-SOCS1-KIR.

Methods: We stimulated J774A.1 cells with lipopolysaccharide (LPS) in the presence of R9-SOCS1-KIR or its inactive control peptide. Effect on inflammatory pathways was followed by the nuclear translocation of nuclear factor κ B p65 subunit and phosphorylated-p38. Synthesis of inflammatory markers induced by LPS was tested by reverse transcriptase polymerase chain reaction, Western blot analysis, and ELISA of cell supernatants. We monitored effects on the barrier properties of a differentiated ARPE-19 monolayer treated with LPS. We treated C57BL/6 mice topically with either R9-SOCS1-KIR or vehicle and injected their eyes intravitreally with LPS. Eyes were analyzed by funduscopy, fluorescein angiography, optical coherence tomography, histology, Western blotting, multiplex enzyme-linked immunosorbent assay, and flow cytometry.

Results: Treatment with R9-SOCS1-KIR resulted in suppression of signaling through nuclear factor κ B and p-p38 pathways. R9-SOCS1-KIR suppressed the expression of inflammatory genes, the secretion of inflammatory makers such as nitric oxide, and IL-1 β induced by LPS. Increased permeability of retinal pigment epithelial cell monolayers was prevented. Corneal administration of R9-SOCS1-KIR blocked the acute inflammation observed in LPS-injected mouse eyes.

Conclusions: Treatment with R9-SOCS1-KIR alleviated the inflammatory responses in cell culture. Topical delivery of this peptide on mouse eyes protected against LPS-induced damage.

Translational Relevance: Topical delivery of R9-SOCS1-KIR peptide allows the patient to self-administer the drug, while preventing any systemic effects on unrelated organs.

Introduction

Uveitis is a heterogeneous group of diseases that accounts for 10% to 15% of all cases of blindness globally.¹ Infections cause some forms of uveitis, whereas autoimmunity or autoinflammation, which involve T cells, can give rise to noninfectious uveitis.² The disease can affect all age groups, thus

causing a significant socioeconomic burden. Aside from the external triggers, a dysregulated microbiome (intestinal, salivary, or ocular) is also associated with uveitis,^{3–5} blurring the distinction between infectious and noninfectious uveitis. Current treatment of acute uveitis includes the topical, periocular, or systemic administration of corticosteroids, but their use may result in undesirable side effects, such as decreased resistance to infection, decreased

wound healing, increased intraocular pressure, and an increased incidence of glaucoma and cataracts.⁶

Since its first demonstration in 1980, endotoxin-induced uveitis (EIU) has been a widely used animal model to study the acute ocular inflammation.⁷ The small animal EIU models mimic the human disease in many ways and have been useful in understanding the mechanism of the disease and in developing therapeutics to mitigate pathological effects of uveitis.⁸ EIU, initiated by the injection of lipopolysaccharide (LPS), is associated with the breach of the blood–retinal barrier and the ensuing infiltration of inflammatory cells and induction of inflammatory mediators.

Suppressor of cytokine signaling (SOCS) is a group of eight intracellular proteins that are induced in response to cytokines and serve as their feedback inhibitors.^{9,10} In contrast with the other checkpoint inhibitors, such as programmed cell death 1, programmed cell death 1 ligand, and CTLA4 that are restricted to the immune cells,¹¹ SOCS proteins are effective in many somatic cells, including those in many compartments of the eye.^{12,13} SOCS1 and SOCS3 possess a kinase inhibitory region (KIR) near their N-termini that are involved in suppression of signaling emanating from JAK/STAT and Toll-like receptor (TLR) 2/4 pathways. We have shown that the KIR of SOCS1 that spans from amino acids 53 to 68 is sufficient to block signaling from JAK/STAT and TLR2/4 pathways.¹⁴ Attachment of polyarginine (R9) to this peptide allows it to cross the plasma membrane. The peptide thus generated is denoted R9-SOCS1-KIR. We have recently shown that R9-SOCS1-KIR can protect the eyes of mice in experimental autoimmune uveitis (EAU), as both a prophylactic and a therapeutic.¹⁵ In addition to EAU reported earlier, we show herein that R9-SOCS1-KIR decreased the inflammatory signaling caused by LPS in a macrophage cell line and damage to retinal pigment epithelial cells in culture. Topically administered peptide protected mice against EIU.

Methods

Cell Culture

Mouse macrophage cell line, J774A.1 (ATCC, TIB-67) was grown in Dulbecco's Modified Eagle's Medium (DMEM) medium containing 10% fetal bovine serum (FBS) and 1% each of penicillin and streptomycin in a humidified incubator at 37°C and 5% CO₂. ARPE-19 cells (ATCC, 2302) were grown as described previously.¹⁵

Peptide Synthesis

The peptide, R9-SOCS1-KIR, RRRRRRRRRD-THFRTRSHSDYRRI, and its inactive control peptide with the sequence, RRRRRRRRRD THARTARSHSDYRRI, which was denoted as R9-SOCS1-KIR2A, were synthesized chemically by GenScript (Piscataway, NJ) to 95% purity. The R9 sequence was included in these peptides to allow their penetration across the plasma membrane. Sterile phosphate-buffered saline (PBS) was the diluent for these peptides.

Immunohistochemistry

J774A.1 or ARPE-19 cells were grown overnight in cell culture slides, and then the medium was changed to medium with 1% FBS. To test the impact of LPS, cells in low serum media were incubated with 20 μM R9-SOCS1-KIR or with 20 μM R9-SOCS1-KIR2A (control) for an hour followed by exposure to *Escherichia coli* LPS (Sigma Aldrich, St. Louis, MO) at 100 ng/mL for 30 minutes. To differentiate ARPE-19 cells to form tight junctions, we grew cells in DMEM containing 1% FBS for 4 weeks. Differentiated retinal pigment epithelial cell (RPE) cells were incubated with R9-SOCS1-KIR or with R9-SOCS1-KIR2A at 20 μM for 3 hours and then incubated with LPS for 48 hours. We added zona occludens 1 (ZO-1) antibodies to the monolayer, followed by imaging with fluorescently tagged secondary antibody as described previously.¹⁵ Cells were imaged either with a Leica DMi8 or with a Keyence BZ-X700 fluorescence microscope.

Analysis of Transcript Levels

J774A.1 cells were grown to confluence in a 12-well plate. The next day, the medium was changed to low serum and cells were exposed to 20 μM R9-SOCS1-KIR for 1 hour followed by 100 ng/mL of LPS for 4 hours. We washed the cells in PBS and then extracted RNA using Trizol reagent (Invitrogen), followed by Direct-zol RNA kit from Zymo Research. We used the iScript kit from Bio-Rad (Hercules, CA) to synthesize complementary DNA. The polymerase chain reaction (PCR) mixture and conditions are identical to those described in our earlier article.¹⁵ The sequence of PCR primers, synthesized by Eurofins is listed in Table. A similar procedure was followed for extraction of RNA and quantitative PCR for the retinae isolated from mouse eyes. We normalized gene expression to β-actin. We used the $\Delta\Delta C_t$ method to determine the

Table. Nucleotide Sequence of PCR Primers Used for Quantitative PCR

1. IL-1 β -F: GCAGCAGCACATCAACAAGAGC
2. IL-1 β -R: TCGGAGCCTGTAGTGCAGTTG
3. IL-6-F: GTTGCCTTCTGGGACTGATG
4. IL-6-R: GCACAACTCTTTTCTCATTTCACAG
5. MCP-1-F: TCTGGGCTGTGTTCCACAGTT
6. MCP-1-R: CCTCTCTCTTGAGCTTGGTGAC
7. TNF α -F: CTGTAGCCACGTCGTAGCA
8. TNF α -R: GAGGAGGTTGACTTTCTCTCTGG
9. iNOS-F: GGAGCGAGTTGTGGATTGTC
10. iNOS-R: CTGAACTTCCAGTCATTGACTCTGAG
11. COX-2-F: GAAGTCTTTGGTCTGGTGCCTG
12. COX-2-R: GAAACTGTTTGAAGCTGACTCCTGG
13. β -actin-F: CGAGCACAGCTTCTTTGCA
14. β -actin-R: TTCCCACCATCACACCCTGG

F, forward; R, reverse; MCP-1, monocyte chemoattractant protein-1; iNOS: inducible nitric oxide synthetase; TNF, tumor necrosis factor.

relative expression of target genes in different treatment groups.¹⁶

Macrophage Activation Assay

After growth overnight, mouse macrophage cells (J774A.1) were incubated with DMEM containing 1% FBS and exposed to varying concentrations of R9-SOCS1-KIR or to R9-SOCS1-KIR2A at 20 μ M for 1 hour, followed by incubation with LPS at 1 μ g/mL for 24 hours. We used culture supernatants to measure nitrite using Greiss reagent, according to the manufacturer's protocol (Alexis Biochemicals, Plymouth Meeting, PA). We estimated nitric oxide concentration from a standard curve generated in parallel using sodium nitrite as a substrate.

Enzyme-Linked Immunosorbent Assay (ELISA) for IL-1 β

The J774A.1 cells were grown overnight and then placed in DMEM containing 1% FBS and treated LPS (1 μ g/mL) in the presence of R9-SOCS1-KIR at varying concentrations, or control peptide (30 μ M) for 24 hours. Supernatants from J774A.1 cells were used in triplicate for an ELISA to measure IL-1 β using a kit from PeproTech (Rocky Hill, NJ), as described elsewhere.¹⁷

Western Blot Analysis

The J774A.1 cells were incubated with 20 μ M R9-SOCS1-KIR or R9-SOCS1-KIR2A for 1 hour,

followed incubation with LPS (1 μ g/mL) for 24 hours. Equal amounts of proteins from cell extracts from these treatments were run on a 12% SDS-polyacrylamide gel and blotted to a polyvinylidene difluoride membrane using an iBlot system (ThermoFisher, Waltham, MA). The membrane was soaked in the blocking buffer from LiCor BioSciences (Lincoln, NE) for 1 hour followed by overnight incubation with antibodies to cyclo-oxygenase (COX-2) and α -tubulin (as an internal control) at 4°C. We rinsed the membrane 4 times with PBS 0.1% Tween 20 and incubated with the appropriate IR dye-labeled secondary antibodies (1:5000 dilution in blocking buffer) for 30 minutes. The membrane was rinsed multiple times in blocking buffer and then scanned with an Odyssey infrared imaging system (LiCor BioSciences). The experiment was repeated two more times with cells treated similarly and cell extracts from these were used for Western blots. The intensity of the COX-2 band and that of corresponding α -tubulin band from three independent experiments was measured using image J (NIH) software and averaged. The relative intensity in untreated cells was taken as 1. One-way analysis of variance followed by a post hoc Tukey's test for multiple comparisons was used to determine the statistical significance between different treatments.

Measurement of Transepithelial Resistance

We plated ARPE-19 cells on transwell inserts (Greiner-Bio-one) in DMEM/F-12 and grew them overnight. The medium was changed to DMEM/F12 plus 1% FBS and cells were grown for 4 weeks, changing the medium twice per week. After this period, we incubated cells on the transwells with R9-SOCS1-KIR at 20 μ M for 3 hours followed by exposure to LPS (1 μ g/mL) for 48 hours. We measured transepithelial electrical resistance (TEER) using an EVOM2 voltohmmeter (World Precision Instruments). We placed inserts into the EVOM2 chamber filled with DMEM/F-12 medium. We calculated transepithelial resistance by subtracting the value of a blank transwell filter from the value of the filters with plated cells, and presented as average Ohm.cm² \pm standard deviation.

Induction of EIU and Topical Administration of Peptides

We housed mice (C57Bl/6 mice from Taconic) in a room with a 12-hour light–12-hour dark cycle. We conducted experiments in accordance with the ARVO Statement for the Use of Animals in Ophthalmic and Vision Research. Six to eight week old male and female

mice (10 per group) were pretreated on days -2 , -1 , and 0 by instillation in the eye of $15\ \mu\text{g}$ R9-SOCS1-KIR dissolved in $2\ \mu\text{L}$ PBS or control peptide. Mice were held by the scruff for five minutes for the peptide delivery across cornea to prevent the mouse from wiping out the delivered peptide. On day 0 , mice were injected intravitreally with $125\ \text{ng}$ in $1\ \mu\text{L}$ of *E coli* LPS in both eyes. One day after LPS treatment, peptides were administered as described in this paragraph and mice were used for analysis as follows.

Retinal Imaging and Cell Counting

We followed the same procedures as we have described earlier for digital fundus microscopy and spectral domain optical coherence tomography.¹⁷ To measure the thickness of the outer nuclear layer and the total retina, four measurements equidistant from the optical nerve head were recorded from each eye. We averaged the outer nuclear layer thickness measurements from both eyes of each animal and then calculated the mean thickness of each treatment group.

We used ImageJ software (<https://imagej.nih.gov/ij/>) to count cells infiltrating the vitreous. The area corresponding with the vitreous was marked, and reflective spots corresponding to infiltrating cells were converted into binary images. To determine the number of cells in each area we used the count particles function of ImageJ as described by Ridley et al.¹⁸ We averaged the infiltrating cells in both eyes of each mouse and compared the average number of infiltrating cells in eyes from mice treated with R9-SOCS1-KIR or with R9-SOCS1-KIR2A.

Histopathology

One day after administering LPS, we humanely euthanized the mice. We then enucleated their eyes and placed them in 4% paraformaldehyde at 4°C overnight. Thereafter, eyes were placed in PBS and embedded in paraffin to prepare for sectioning. Sectioning was through the cornea–optic nerve axis, at a thickness of $12\ \text{mm}$. We collected eight step sections on different slides. We stained slides with hematoxylin and eosin to visualize the number of infiltrating cells and the structure of retina by light microscopy.

Fluorescein Angiography

Mice anesthetized with a mixture of ketamine ($95\ \text{mg/kg}$) and xylazine ($5\text{--}10\ \text{mg/kg}$) by intraperitoneal injection and were injected intraperitoneally with $50\ \mu\text{L}$ of 10% sodium fluorescein. Each mouse was

held on its side on the platform of a Micron III retinal imaging microscope and imaged using fluorescein filter system.

Retinal Protein Extraction and Analysis

Mouse retinae were squeezed out of the eyeball and collected in $100\ \mu\text{L}$ of lysis buffer ($50\ \text{mM}$ Tris-HCl [pH 8.0], $150\ \text{mM}$ NaCl, 1% NP-40, and protease inhibitor cocktail). Retinae were homogenized by sonication twice for 20 seconds each, followed by centrifugation at $12,000\times g$ for 2 minutes. Clear supernatants were collected and used for protein estimation, followed by dilution to $1\ \mu\text{g}/\mu\text{L}$. Twenty micrograms each were used for Western blot analysis as described elsewhere in this article.

Quantitation of Inflammatory Markers by Multiplex ELISA (MagPix)

Protein extracts from harvested retinae as described elsewhere in this article were diluted to $1\ \mu\text{g}/\mu\text{L}$. Twenty-five micrograms each of the samples in duplicate were taken to quantitate five inflammatory markers using ProcartaPlex Multiplex Immunoassay reagents manufactured by ThermoFisher, following the manufacturer's instructions. Samples or standards were mixed with magnetic beads and incubated overnight at 4°C with shaking. Beads were washed with the wash buffer using a handheld magnetic plate. Detection antibody and streptavidin–phycoerythrin were added and incubated for 30 minutes, followed by washing. Samples were taken in reading buffer and analyzed in a Luminex MagPix instrument and xPONENT software (v4.3, Luminex, Austin, TX). Multiplex analysis software (v5.1, Millipore, St. Louis, MO) was used to convert the data for quantitation.

Generation of Retinal Single-Cell Suspension

Retinae harvested from mice treated with R9-SOCS1-KIR or control group and injected with LPS ($n = 5$ each) were used to obtain single cell suspension using the reagents from the papain dissociation system from Worthington Biochemicals (Lakewood, NJ) as per manufacturer's protocol. Briefly, harvested retinae were placed in $500\ \mu\text{L}$ of papain solution ($20\ \text{U/mL}$ papain, 0.005% DNase in Earle's Balanced Salt Solution) and were incubated in a Thermomixer (Eppendorf, Enfield, CT) for 45 minutes at 37°C and shaking at 700 rpm. Afterwards retinae were further dissociated by pipetting 10 times with a

micropipette, followed by centrifugation at $300\times g$ for 5 minutes. The supernatant was removed, and the cell pellet was resuspended in 500 μL of resuspension solution (diluted ovomucoid, 0.005% DNase in Earle's Balanced Salt Solution). The resuspended cell suspension was carefully overlaid on top of 600 μL of ovomucoid solution followed by centrifugation at $300\times g$ for 5 minutes. The supernatant was removed, and the cell pellet was resuspended in 500 μL of cell staining buffer from Biolegend (San Diego, CA). Finally, cell suspension was passed through a 70- μm cell strainer.

Analysis of Retinal Inflammatory Cells by Flow Cytometry

Retinal single cell suspensions were counted using a hemocytometer and diluted to 10^6 cells/mL using cell staining buffer. Samples were then aliquoted in 1.5 mL tubes at 100 μL (10^5 cells) per tube. The remaining tubes received either 1 μL of the indicated antibody or 1 μL of each antibody (triple stained). These samples were incubated at 4°C in the dark for 1 hour. Afterward, 400 μL of cell staining buffer was

added to each tube, and these were centrifuged at $300\times g$ for 5 minutes. The supernatant was removed and the cell pellet was then resuspended in 500 μL of Fluoro Fix Buffer from Biolegend and incubated in the dark for 30 minutes. Cells were then centrifuged at $300\times g$ for 5 minutes, and the supernatant was removed. Cells were washed once with 500 μL of cell staining buffer followed by a centrifugation as done previously. Finally, the cell pellet was resuspended in 500 μL of cell staining buffer and stored at 4°C until read on a FACS analyzer. Unstained fixed cells were used to set the appropriate forward and side scatter gating, and single stained samples were used to determine the proper compensation. A total of 20,000 gated events were acquired for analysis.

Statistical Analysis

Experiments in cell culture are presented as average \pm standard deviation. We used the Student unpaired two-tailed *t*-test to compare the mean transcript levels treated and untreated cells. For studies in mice, results are presented as average \pm standard deviation. For

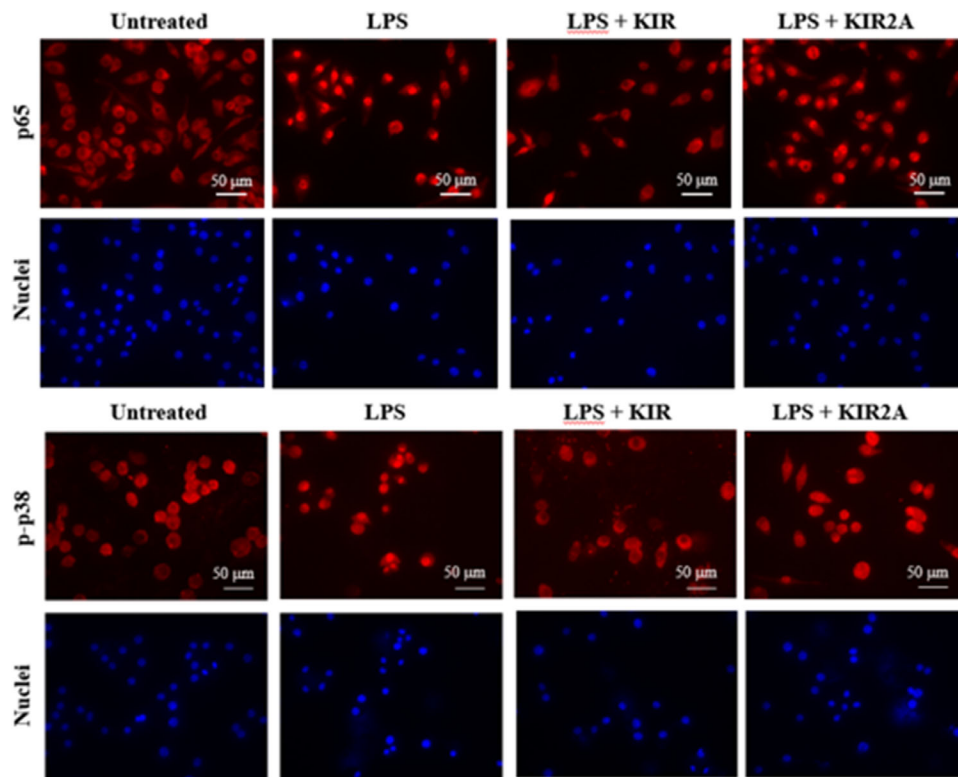


Figure 1. R9-SOCS1-KIR dampens NF- κ B (A) and MAP kinase (B) signaling in J774A.1 cells. J774A.1 cells were seeded in an eight-well cell culture slide and grown overnight. Cells were incubated with R9-SOCS1-KIR (KIR) or with R9-SOCS1-KIR2A (KIR2A) peptide at 20 μM for 1 hour, followed exposure to LPS (100 ng/mL) for 30 minutes. Untreated cells or those treated with LPS (100 ng/mL for 30 minutes) were used for comparison. Cells were doubly stained with an antibody to p65 (active subunit of NF- κ B, A), or MAP kinase p-p38 (B), and DAPI (nuclei, bottom row) and imaged by fluorescence microscopy.

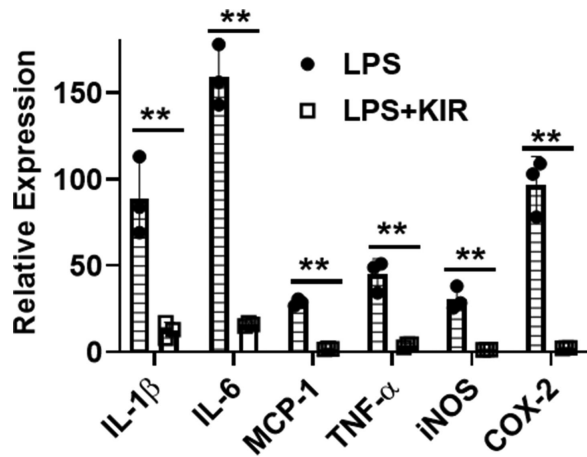


Figure 2. R9-SOCS1-KIR suppresses the inflammatory mediators induced by LPS in J774A.1 cells. J774A.1 cells were treated with R9-SOCS1-KIR (20 μ M) for 1 hour followed by treatment with LPS (100 ng/mL) for 4 hours. RNA was extracted, converted into complementary DNA (cDNA), and used for quantitative PCR. Analysis was done using β -actin as an internal control. Relative expression (versus β -actin) \pm SD, for both the LPS and LPS and SOCS1-KIR treated cells versus untreated cells is presented. The relative expression (vs β -actin) in untreated cells was arbitrarily taken as 1. The results represent the average of three independent experiments. The Student *t*-test for statistical difference showed a *P* value of 0.001 between LPS and LPS plus SOCS1-KIR treated cells.

experiments in which multiple samples were compared, we used one-way analysis of variance followed by Tukey's multiple comparison test or the Holm-Šidák test to evaluate statistical significance. GraphPad Prism 8.2.1 software (San Diego, CA) was used to analyze statistical significance. A *P* value of less than 0.05 was considered statistically significant.

Results

R9-SOCS1-KIR Dampens the Signaling From TLR4 Induced by LPS

Macrophages play a crucial role in inflammatory diseases, beginning with their role in innate immunity followed by the initiation and modulation of adaptive immune response involving phagocytosis as well as the secretion of proinflammatory cytokines. We have used a mouse macrophage cell line, J774A.1, to evaluate the protective effect of R9-SOCS1-KIR against the damage caused by LPS. Because LPS is known to act through TLR4, leading to the activation of nuclear factor κ B (NF- κ B) and MAP kinase p38 pathways,^{19,20} we tested its effect on J774A.1 cells. The J774A.1 cells grown on microscopic slides were pretreated with R9-SOCS1-KIR, or its inactive control peptide

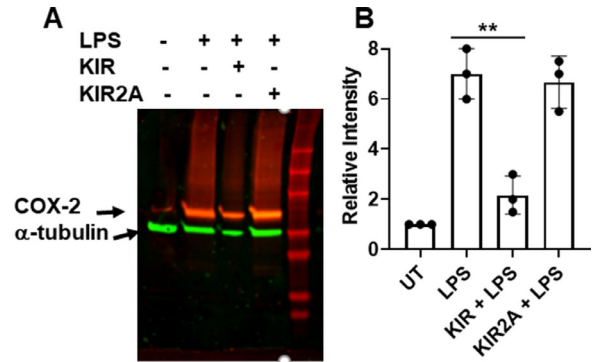


Figure 3. LPS-induced expression of COX2 in J774A.1 cells is downregulated by R9-SOCS1-KIR. Equal amounts of proteins from cell extracts from J774A.1 cells treated with R9-SOCS1-KIR or the control peptide (both at 20 μ M) for 1 hour, followed by treatment with LPS (1 μ g/mL) for 24 hours were separated by electrophoresis, transferred to polyvinylidene difluoride membrane, and probed with antibodies to COX-2 and α -tubulin. The membrane was washed and incubated with corresponding IR dye secondary antibodies. The membrane was washed and scanned with an Odyssey infrared imaging system (LiCor BioSciences). (A) The experiment was repeated two more times with cells treated similarly and cell extracts from these were used for Western blots. The intensity of the COX2 band and that of corresponding α -tubulin band from three independent experiments was measured using image J (NIH) software and averaged. The relative intensity in untreated cells was taken as 1, and the relative intensities for the other treatments is shown in (B). One-way analysis of variance (ANOVA) followed by Tukey's test for multiple comparisons showed significant differences between different treatments, with a *P* value of 0.001 for LPS versus LPS and SOCS1-KIR.

R9-SOCS1-KIR2A at 20 μ M for 1 hour, followed by treatment with LPS at 100 ng/mL for 30 minutes. Cells were then fixed, permeabilized, and stained with an antibody to the active subunit of NF- κ B, p65, or the activated MAP kinase, phosphorylated-p38 (p-p38). Cells were also stained with DAPI to visualize nuclei, and viewed in a fluorescence microscope (Figs. 1A and 1B). Treatment with LPS resulted in nuclear translocation of p65 (Fig. 1A), as well as p-p38 (Fig. 1B). The nuclear translocation p65 or p-p38 was inhibited in the presence of R9-SOCS1-KIR, although there was no effect on translocation in the presence of the control peptide, suggesting the specificity of R9-SOCS1-KIR to dampen NF- κ B and p-p38 signaling.

Synthesis and Secretion of LPS-Induced Inflammatory Markers Is Suppressed by R9-SOCS1-KIR

We used J774A.1 cells to test the effect of LPS induction on the synthesis of messenger RNA (mRNA) for inflammatory markers, and the preventive

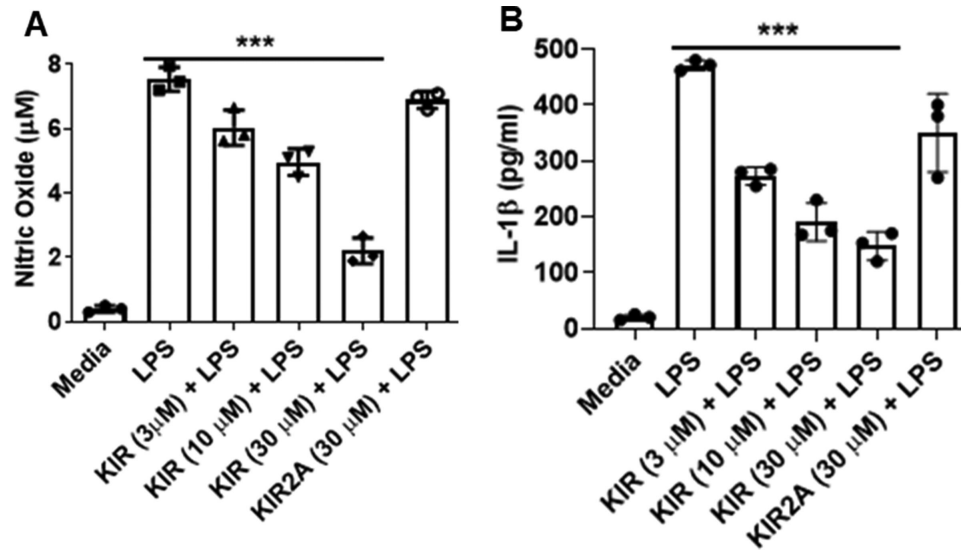


Figure 4. SOCS1-KIR suppresses the production of nitric oxide (NO) and IL-1 β from LPS-induced macrophage cell line, J774A.1. The J774A.1 cells were seeded in a 24-well plate and grown overnight. They were taken in low serum media and treated with increasing concentrations of SOCS1-KIR (KIR), or the control peptide (KIR2A) for 1 hour followed by treatment with LPS (1 μ g/mL) for 24 hours. (A) Supernatants were harvested and used in triplicate to quantitate NO using Griess reagent. (B) Supernatants were harvested and used in triplicate for quantitation of IL-1 β by ELISA. Bars represent the average \pm SD. Results are representative of three independent experiments. One-way analysis of variance (ANOVA) followed by Tukey's test for multiple comparisons showed significant differences between different treatments, with a P value of 0.0001 for LPS versus LPS and 30 μ M of SOCS1-KIR.

effect of R9-SOCS1-KIR. RNA was extracted from J774A.1 cells treated with LPS (100 ng/mL) for 4 hours in the presence or absence of R9-SOCS1-KIR and was used to synthesize complementary DNA to quantitate the relative expression of the following inflammatory markers. IL-1 β , IL-6, monocyte chemoattractant protein 1 (MCP-1), tumor necrosis factor- α , inducible nitric oxide synthetase, and COX-2. Treatment with LPS resulted in a 30- to 150-fold induction of these mediators of inflammation (Fig. 2). The simultaneous presence of R9-SOCS1-KIR decreased the expression of these mediators by 85% to 95%. In the eye, the induction of these proteins can cause an influx of macrophages and neutrophils and lead to the disruption of the blood-retinal barrier.²¹

COX-2 is one of the major mediators of LPS-induced inflammation. To evaluate the effect on the production of COX-2, we used the cell extracts from J774A.1 cells, under different treatments and analyzed by Western blotting (Fig. 3A). One day after the treatment of J774A.1 cells with LPS, there was a seven-fold increase in the synthesis of COX-2, which was suppressed by 70% in R9-SOCS1-KIR-treated cells. The experiment was repeated two more times with cells treated similarly and cell extracts from these were used for Western blots. The intensity of the COX2 band and that of corresponding α -tubulin band

from three independent experiments was measured using image J (NIH) software and averaged. The relative intensity in untreated cells was taken as 1, and the relative intensities for the other treatments is shown in Figure 3B. The control peptide treatment did not lead to a significant decrease, suggesting the specificity of action of R9-SOCS1-KIR in downregulating the production of COX-2 at the protein level.

To verify the consequence of the inhibition inflammatory gene expression, we followed the effect R9-SOCS1-KIR on the release of inflammatory markers NO and IL-1 β . We pretreated J774A.1 cells with R9-SOCS1-KIR at different concentrations followed by treatment with LPS at 1 μ g/mL for 24 hours. Supernatants from these cells were harvested and quantitated for NO and IL-1 β , using Griess reagent to detect NO and ELISA to measure IL-1 β . Secretion of NO induced by LPS was inhibited in a dose-dependent manner in the presence of R9-SOCS1-KIR ($P = 0.02$), but not with the inactive control peptide (Fig. 4A). Secretion of IL-1 β was also inhibited in a dose-dependent manner in the presence of R9-SOCS1-KIR ($P = 0.01$), but not in the presence of control peptide (Fig. 4B), suggesting the specificity of R9-SOCS1-KIR in suppressing the release of inflammation-inducing agents in the media.

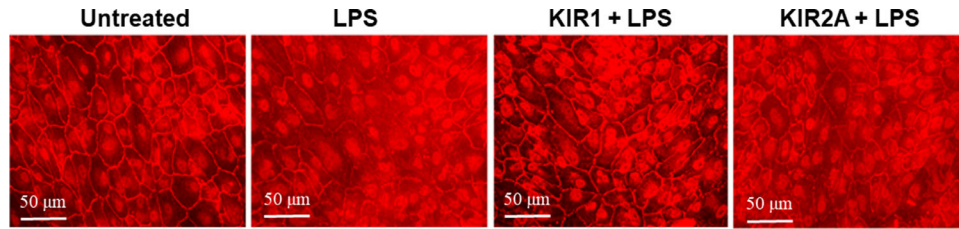


Figure 5. Cell-penetrating SOCS1 peptide prevents loss of tight junctions. ARPE-19 cells grown for four weeks in low serum medium were left untreated or treated with SOCS1-KIR or control peptide (both at 20 mM for 3 hr), followed by exposure to LPS (1 μ g/mL), for 48 hours. Cells were incubated with an antibody to ZO-1 and viewed in a fluorescence microscope. The distribution of ZO-1 around the cells was disrupted by LPS, but protected in the presence of SOCS1-KIR peptide (KIR), but not with the control peptide (KIR2A). The images were taken at an original magnification of $\times 40$.

Protection Against Damage to Barrier Properties of ARPE-19 Cells by R9-SOCS1-KIR

The RPE serve several crucial roles, including that of maintaining the blood–retinal barrier.²² ARPE-19 cells are a spontaneously derived human RPE cell line.²³ The induction of NO, COX2, and the inflammatory cytokines by LPS, as noted elsewhere in this article, results in the disruption of blood–retinal barrier during EIU.²¹ Therefore, we tested the effect of LPS treatment on ARPE-19 cells. ARPE-19 cells were grown in low serum medium for 4 weeks until they had acquired a cobblestone-structured morphology. Cells were pretreated with R9-SOCS1-KIR or the control peptide (both at 20 μ M for 3 hours), followed by treatment with LPS (1 μ g/mL for 48 hours). Cells were stained with an antibody to ZO-1, which is one of a group tight junction proteins that regulate cell permeability. Untreated cells or those treated with R9-SOCS1-KIR alone showed a continuous staining along the cell surfaces (Fig. 5). This continuous distribution was disrupted when the cells were treated with LPS, whereas in the simultaneous presence of R9-SOCS1-KIR, this damage was prevented. The inactive control peptide was not able to protect against the damage caused by LPS.

The loss of tight junction proteins affects the TEER across the RPE layer. ARPE-19 cells grown in low serum medium in 24-well transwell plates for 4 weeks as described elsewhere in this article for ZO-1 staining were treated with LPS in the presence or absence of R9-SOCS1-KIR. The measurement of TEER across the APRE-19 cells using a voltohmmeter revealed a 70% decrease with LPS treatment ($P = 0.001$), whereas the simultaneous presence of R9-SOCS1-KIR resulted in 28% loss of TEER ($P = 0.001$) (Fig. 6). The SOCS1-KIR peptide, on its own, did not have any considerable effect on TEER. Thus, R9-SOCS1-KIR protected against the distribution of ZO-1 along the cell membrane as

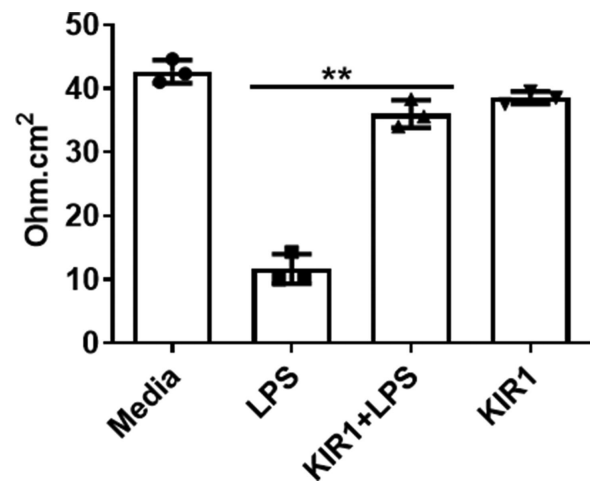


Figure 6. Cell-penetrating SOCS1 peptide prevents LPS-induced reduction in TEER. ARPE-19 grown in transwell plates in low serum medium were incubated with 20 μ M SOCS1-KIR for 3 hours, and then incubated with LPS (1 μ g/mL) for 48 hours as indicated. Transepithelial resistance (TEER) was measured in triplicate, with a voltohmmeter. One-way analysis of variance (ANOVA) followed by Tukey's multiple comparisons indicated a P value of 0.001s between LPS and LPS and SOCS1-KIR treated cells.

well as the loss of electrical resistance across the membrane.

Topical Administration of R9-SOCS1-KIR Protected Mice Against LPS-Induced Uveitis

LPS, an endotoxin from gram-negative bacteria initiates EIU. We administered LPS intravitreally in C57BL/6 mice to generate EIU and investigated the protective effect of R9-SOCS1-KIR after this inflammatory insult. Two groups of C57BL/6 mice ($n = 10$ in each, both male and female) were injected with 125 ng per eye of *E coli* LPS in both eyes. One group of mice was treated on the corneal surface of both eyes with 15 μ g per eye (in 2 μ L) of R9-SOCS1-KIR peptide on days -2 , -1 , and 0, as well as day 1 after the LPS

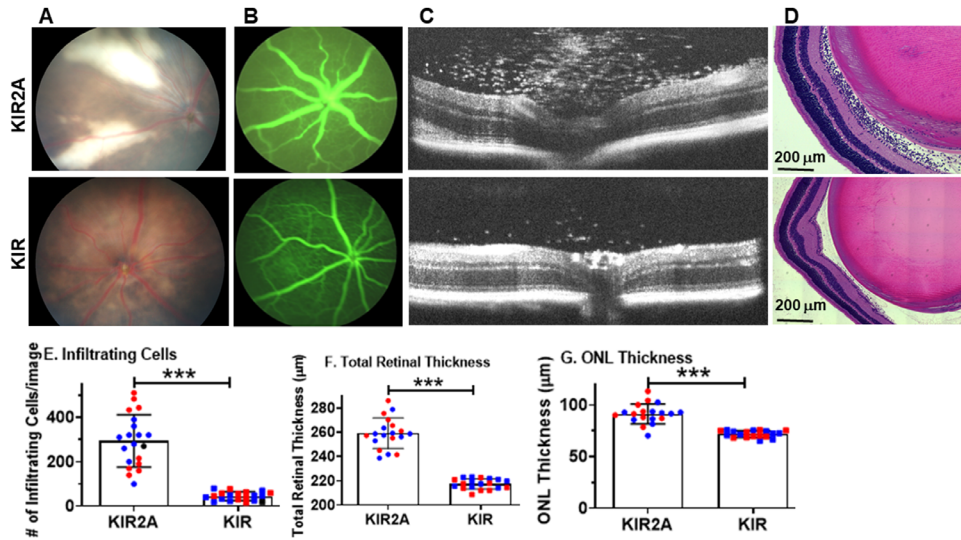


Figure 7. Topical treatment with R9-SOCS1-KIR protects mouse eyes against the damage caused by EIU. C57BL/6 mice (both male and female, 6–8 weeks old, $n = 10$ in each group) were used for administering R9-SOCS1-KIR, or control peptide (both at 15 µg in 2 µL) by eye dropping in both eyes on days -2, -1, and 0. On day 0, mice were injected intravitreally with *E coli* LPS (125 ng in 1 µL) in both eyes. Peptide treatment was done again one day after LPS injection, followed by funduscopy (A), fluorescein angiography (B), and spectral domain optical coherence tomography (C). Eyes were enucleated, fixed, sectioned and stained with hematoxylin and eosin and observed in a microscope at an original magnification of $\times 5$ (D). The number of infiltrating cells/image in female and male mice was carried out as described in the Methods ($n = 10$ in each group) (E). Retinal thickness (F) and outer nuclear layer (ONL) (G), were measured in the control and treatment groups ($n = 10$ each group), and plotted for female (blue dots) and male mice (red dots). P values between the control and SOCS1-KIR groups for infiltrating cells/image, total retinal thickness and ONL thickness were less than 0.0001. The thickness of each layer was measured using the segmentation of Diver 2.0 software from Leica Microsystems. The Student t -test was used to measure the statistical significance.

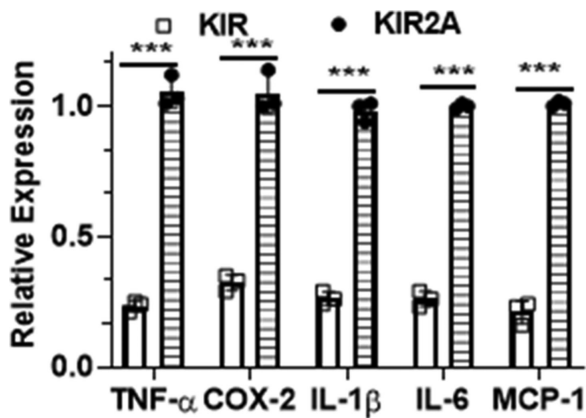


Figure 8. R9-SOCS1-KIR treatment decreased the levels of transcripts of inflammatory mediators. Retinae isolated from mice treated with R9-SOCS1-KIR, or its inactive control peptide, SOCS1-KIR2A were used to isolate RNA and synthesize complementary DNA (cDNA) for quantitative reverse transcriptase PCR. Expression levels in control treated mice were arbitrarily taken as 1, and the relative decrease in expression in SOCS1-KIR treated retinae is presented as average \pm SD ($n = 3-4$ mice per group). Averaged values were compared with a two-way analysis of variance (ANOVA) followed by a Holm-Sidak test to identify statistical differences for each target gene between SOCS1-KIR and SOCS1-KIR2A groups.

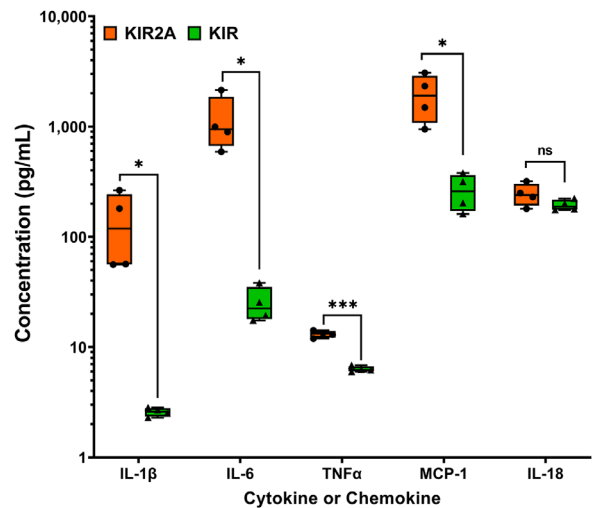


Figure 9. Suppression of inflammatory markers by SOCS1-KIR treatment analyzed by multiplex ELISA. Retinae were harvested from mice 1 day after LPS injection and control or SOCS1-KIR peptide treatments ($n = 4$ in each group). Proteins isolated from the retinae were used to perform multiplex ELISA. Quantification of cytokines and chemokines within the retina lysates of these mice was done. Analyte concentrations were standardized to total amount of protein used in the assay (pg/mg total protein).

injection. The control group was treated similarly with the control peptide, R9-SOCS1-KIR2A. The injection of LPS was done on day 0. One day after LPS injection, digital funduscopy revealed an influx of inflammatory cells, perivascular deposits, engorged blood vessels, and hemorrhage in the control group, whereas the mice treated with R9-SOCS1-KIR showed fewer inflammatory cells and an occasional swollen optic nerve (Fig. 7A). Consistent with this result, fluorescence angiography (Fig. 7B) revealed swollen blood vessels and increased fluorescein leakage in the control eyes. These findings were not observed after treatment with the SOCS1-KIR. Examination by spectral domain optical coherence tomography 1 day after LPS administration showed many infiltrating cells in the optical axis, vitreous, and retina, as well as retinal swelling and/or buckling in the control group (Fig. 7C). In contrast, mice that were given R9-SOCS1-KIR showed fewer inflammatory cells and the retinal structure was not affected. One day after LPS injection, eyes were harvested, fixed, and stained with hematoxylin and eosin (Fig. 7D). A large influx of inflammatory cells in retina and vitreous was seen in the control eyes, whereas there was a considerable decrease in these cells in the SOCS1-KIR-treated eyes. The number of inflammatory cells in B-scans from three areas of the posterior chamber was determined using ImageJ software. In control mice, the average number of infiltrating cells was 280 ± 85 per image, whereas the average in R9-SOCS1-KIR-treated mice was 45 ± 15 per image ($n = 20$; $P < 0.0001$), resulting in a six-fold decrease with the topical administration of the peptide (Fig. 7E). The optical coherence tomography measurements revealed a swelling of retina as well, with the total retina measuring $260 \pm 12 \mu\text{m}$ in control versus $217 \pm 4 \mu\text{m}$ in the SOCS1-KIR-treated mice (Fig. 7F). The outer nuclear layer in the control retina measured at $91 \pm 9 \mu\text{m}$, whereas in the SOCS1-KIR peptide treated ones, it was $72 \pm 3 \mu\text{m}$ ($n = 20$; $P < 0.0001$) (Fig. 7G). The structural damage caused by LPS was thus prevented by R9-SOCS1-KIR peptide. As noted in Figures 7E–G, there was no difference in the severity of the disease after LPS induction or therapeutic effects of SOCS1-KIR between male and female mice.

We extracted RNA from the retinae of mice treated with SOCS1-KIR or control peptides to quantitate the relative expression of inflammatory markers (tumor necrosis factor- α , COX-2, IL-1 β , IL-6, and monocyte chemoattractant protein-1) by quantitative PCR with gene-specific primers. Expression in the eyes treated with the control peptide, SOCS1-KIR2A was arbitrarily taken as 1. The retinae from mice treated with R9-SOCS1-KIR revealed a three- to five-fold decrease in

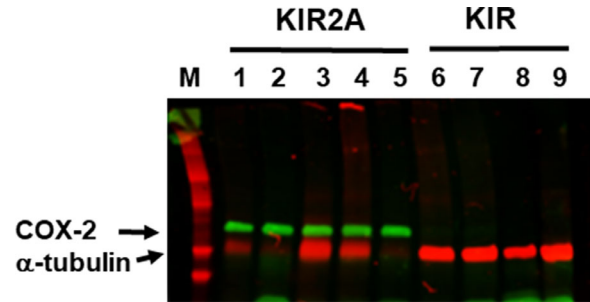


Figure 10. Expression of COX-2 noted in LPS injected retinae is reduced by SOCS1-KIR treatment. Proteins (20 μg each from isolated from retina of LPS injected eyes treated with the control [$n = 5$] or SOCS1-KIR [$n = 4$] peptide) were separated on a 5% to 15% SDS-PAGE, transferred to polyvinylidene difluoride membrane and probed with antibodies to COX-2 and α -tubulin as an internal control. A strong band for COX-2 was observed in control eyes, but this was not seen in the eyes treated with SOCS1-KIR.

the level of these transcripts ($n = 3-4$; $P < 0.0001$) (Fig. 8), suggesting an anti-inflammatory role for the R9-SOCS1-KIR peptide. To verify that the suppressed transcription of these inflammatory markers in retina was reflected in a decrease at the protein level, we isolated proteins from the control and SOCS1-KIR-treated retinae ($n = 4$ each) and carried out multiplex ELISA assay using MagPix as shown in Figure 9. The level of IL-1 β decreased from $140 \pm 100 \text{ pg/mL}$ in the control group to $2.58 \pm 0.2 \text{ pg/mL}$ after treatment with R9-SOCS1-KIR, showing a 50-fold decrease ($P = 0.01$). A similar decrease in IL-6 levels was noted, where $1160 \pm 680 \text{ pg/mL}$ in control was reduced to $24.7 \pm 9 \text{ pg/mL}$ ($P = 0.01$) upon treatment with R9-SOCS1-KIR. Tumor necrosis factor- α and monocyte chemoattractant protein-1 were reduced from 13 ± 0.8 to $6 \pm 0.4 \text{ pg/mL}$ ($P = 0.0001$) and $1962 \pm 930 \text{ pg/mL}$ to $264 \pm 100 \text{ pg/mL}$ in control and SOCS1-KIR treated mice, respectively. There was no significant change in the levels of IL-18.

A decrease in the level of COX-2, a major contributor to the inflammation noted in EIU, and tested by reverse transcriptase PCR (Fig. 8) was confirmed by Western blot analysis of the retinal proteins isolated from control or SOCS-KIR peptide groups (Fig. 10). A distinct band for COX-2 was noted in the control group ($n = 5$), whereas the expression of COX-2 was suppressed upon treatment with SOCS1-KIR peptide ($n = 4$).

Retinae isolated from control or SOCS1-KIR-treated mice ($n = 5$ each) were dispersed into single cell suspension and used for multicolor flow cytometric analysis to test the presence of inflammatory cells (Fig. 11). Treatment with SOCS-KIR resulted in a two-fold decrease in macrophages ($P = 0.01$) and neutrophils (not significant), which is consistent

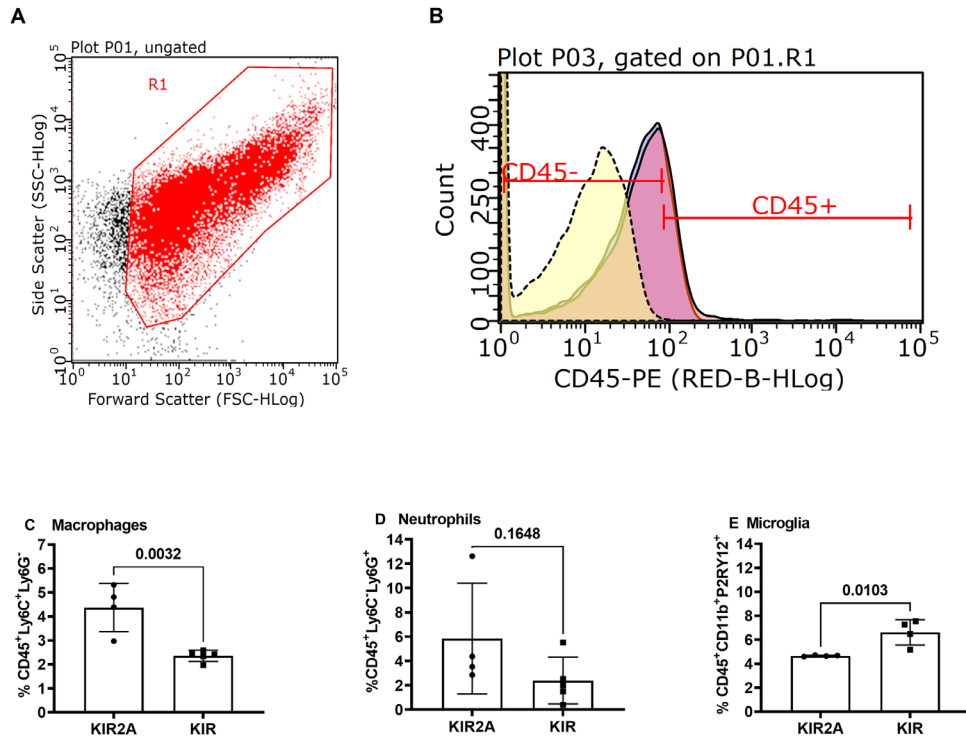


Figure 11. Flow cytometric analysis of inflammatory cells in retinae. Retinal cells isolated from retinae of mice injected with LPS and treated with control or SOCS1-KIR peptide ($n = 5$ each) were stained and separated. Retinal cells were then gated by forward and side scatter (A). Immune cells were identified by the expression of CD45 (B). CD45 positive cells were then evaluated for the expression of macrophage markers (CD45⁺Ly6C⁺Ly6G⁻) (C), neutrophil markers (CD45⁺Ly6C⁻Ly6G⁺) (D), or microglia markers (CD45⁺CD11b⁺P2RY12⁺) (E).

with the decrease in inflammatory markers in the retina noted in the preceding assays. There was a 1.5-fold increase in microglia ($P = 0.01$) upon treatment with SOCS1-KIR. This result may reflect a decrease in surveying microglia (CD45⁺CD11b⁺P2RY12⁺) owing to retinal inflammation in the control group, which was blocked in the SOCS1-KIR-treated group. Decreases in P2RY12 microglial expression have been described in the brain with the development of neurologic diseases.²⁴ Based on previous research with this model, the infiltrating cells are mostly macrophages and neutrophils.^{25,26} An analysis of the retinal structure, inflammatory markers, and inflammatory cells all point to a protective role of topical administration of SOCS1-KIR in preventing the damage caused by LPS-induced uveitis.

Discussion

LPS has been shown to cause the downregulation of SOCS1 and SOCS3 in macrophages,²⁷ and downregulation of SOCS1 in microglia.²⁸ Thus, LPS is not only inducing the inflammatory agents, but also dimin-

ishing molecules that would otherwise have blunted the effect of these inducers. Given this scenario, the use of R9-SOCS1-KIR offers two potential benefits—one is to suppress the effects of inflammation and another is to compensate for the loss of endogenous SOCS1 and 3 from affected cells. KIR of SOCS1 or 3 binds to the phosphotyrosine-containing domains of the JAK2, TYK2, or MyD88 adaptor protein,¹⁴ thereby limiting the signals emanating from the effector molecules that use JAK2, TYK2, or TLR2/4. We and others have shown that the KIR domain of SOCS1 or 3 can act independently of the remainder of the parent molecule.^{14,29} Attachment of a polycationic sequence, such as R9 allows, this peptide to cross the plasma membrane and act as an immunosuppressant molecule. It is noteworthy that the cell penetrating form of SOCS3-KIR exhibited a longer half-life (29 hours), compared with the cell penetrating form of the full-length protein (6.2 hours),²⁹ suggesting that, in addition to functioning independent of the SOCS box, SOCS3-KIR can remain in the cell longer to counter the damage from inflammatory molecules.

LPS is recognized by TLR4, which triggers an inflammatory response with the activation of NF- κ B and MAP kinase, p38.^{19,20} We showed the ability

of R9-SOCS1-KIR to suppress both the NF- κ B and MAP kinase p38 signaling (Fig. 1). LPS-induced synthesis of mRNA for inflammatory markers was suppressed in the presence of R9-SOCS1-KIR (Fig. 2). Consistent with this finding, the secretion of NO and IL-1 β were suppressed (Figs. 4A and 4B). The production of NO leads to the activation of COX-2, which, in turn, produces prostaglandin. This cascade of the formation of inflammatory mediators, beginning with the activation of NF- κ B promoter, is thus blunted in the presence of R9-SOCS1-KIR, as evidenced by suppression of inflammatory mediators at the mRNA level and secreted molecules in cell culture (Figs. 2 and 3), as well the relative expression of specific mRNAs in retinas (Fig. 8). In addition, binding of SOCS1-KIR to Rac1-GTP leads to a decrease in production of reactive oxygen species, and the ensuing activation of inflammasome, NLRP3.³⁰ This effect may have contributed to the downregulation of IL-1 β production noted in the macrophage cell line (Fig. 4B). Although the effects of SOCS1-KIR were tested in a macrophage and a retinal pigment epithelial cell line, it is worth noting that the beneficial effects of SOCS1-KIR are operational in all cells that use the JAK/STAT and TLR2/4 pathways. This includes the infiltrating macrophages and T cells, activated microglia, and neural cells in all compartments of the eye. Thus, when we analyzed the mouse retinae by reverse transcriptase PCR, multiplex ELISA, Western blotting, and multi-color flow cytometry, we noted a decrease in inflammatory markers as well as inflammatory cells, which may have contributed to the resolution of acute ocular inflammation.

We have described the topical administration of a R9-conjugated SOCS-KIR peptide for protection against EIU. We have recently shown that the topical administration of this peptide protected mice against EAU at both the initiator and effector phases.¹⁵ The effectiveness of topical delivery not only allows a patient to self-administer the compound, but it also limits its effects to the site of delivery, preventing systemic effects from an immunosuppressant given systemically. The benefits of topical delivery of a different version of SOCS1-KIR in protecting against diabetic retinopathy³¹ and EAU³² has recently been reported. There have been several other reports of topical delivery of cell-penetrating peptides, including vascular endothelial growth inhibitor,³³ pigment epithelium-derived factor,³⁴ and endostatin.³⁵ These examples may allow a greater acceptance of the topical delivery of therapeutic peptides in treating various ocular indications.

In conclusion, the immunosuppressant and immunoregulatory properties of R9-SOCS1-KIR

resulted in the downregulation of relevant markers of inflammation, protected against the LPS induced breach of blood retinal barrier. More important, topical administration of SOCS-KIR protected mice against the EIU as noted by reverse transcriptase PCR, multiplex ELISA, and flow cytometry analysis. It is possible that a combination of these properties will allow the topical use of R9-SOCS1-KIR in other inflammatory ocular disorders, such as age-related macular degeneration and autoimmune keratitis.

Acknowledgments

Supported by the Shaler Richardson Professorship endowment to ASL and by an unrestricted grant from Research to Prevent Blindness.

Supported in part by NIH SIFAR Grant 1S10OD028476.

The University of Florida been awarded a patent (US 9,951,111B2) governing the SOCS1 agonist used in this study.

Disclosure: **C.M. Ahmed**, (P); **A.P. Patel**, None; **C.J. Ildefonso**, None; **H.M. Johnson**, (P); **A.S. Lewin**, None

References

- Miserocchi E, Fogliato G, Modorati G, Bandello F. Review on the worldwide epidemiology of uveitis. *Eur J Ophthalmol.* 2013;23:705–717.
- Forrester JV, Klaska IP, Yu T, Kuffova L. Uveitis in mouse and man. *Int Rev Immunol.* 2013;32:76–96.
- Heissigerova J, Seidler Stangova P, Klimova A, et al. The microbiota determines susceptibility to experimental autoimmune uveoretinitis. *J Immunol Res.* 2016;2016:5065703.
- Horai R, Caspi RR. Microbiome and autoimmune uveitis. *Front Immunol.* 2019;10:232.
- Rowan S, Taylor A. The role of microbiota in retinal disease. *Adv Exp Med Biol.* 2018;1074:429–435.
- Carnahan MC, Goldstein DA. Ocular complications of topical, peri-ocular, and systemic corticosteroids. *Curr Opin Ophthalmol.* 2000;11:478–483.
- Rosenbaum JT, McDevitt HO, Guss RB, Egbert PR. Endotoxin-induced uveitis in rats as a model for human disease. *Nature.* 1980;286:611–613.

8. Yadav UCS, Ramana KV. Endotoxin-induced uveitis in rodents. *Methods Mol Biol.* 2019;1960:161–168.
9. Yoshimura A, Suzuki M, Sakaguchi R, Hanada T, Yasukawa H. SOCS, inflammation, and autoimmunity. *Front Immunol.* 2012;3:20.
10. Alexander WS, Hilton DJ. The role of suppressors of cytokine signaling (SOCS) proteins in regulation of the immune response. *Annu Rev Immunol.* 2004;22:503–529.
11. Buchbinder EI, Desai A. CTLA-4 and PD-1 pathways: similarities, differences, and implications of their inhibition. *Am J Clin Oncol.* 2016;39:98–106.
12. Ebong S, Yu CR, Carper DA, Chepelinsky AB, Egwuagu CE. Activation of STAT signaling pathways and induction of suppressors of cytokine signaling (SOCS) proteins in mammalian lens by growth factors. *Invest Ophthalmol Vis Sci.* 2004;45:872–878.
13. Chien H, Alston CI, Dix RD. Suppressor of cytokine signaling 1 (SOCS1) and SOCS3 are stimulated within the eye during experimental murine cytomegalovirus retinitis in mice with retrovirus-induced immunosuppression. *J Virol.* 2018;92:e00526–18.
14. Jager LD, Dabelic R, Waiboci LW, et al. The kinase inhibitory region of SOCS-1 is sufficient to inhibit T-helper 17 and other immune functions in experimental allergic encephalomyelitis. *J Neuroimmunol.* 2011;232:108–118.
15. Ahmed CM, Massengill MT, Brown EE, Ildefonso CJ, Johnson HM, Lewin AS. A cell penetrating peptide from SOCS-1 prevents ocular damage in experimental autoimmune uveitis. *Exp Eye Res.* 2018;177:12–22.
16. Livak KJ, Schmittgen TD. Analysis of relative gene expression data using real-time quantitative PCR and the 2(-Delta Delta C(T)) method. *Methods.* 2001;25:402–408.
17. Ahmed CM, Ildefonso CJ, Johnson HM, Lewin AS. A C-terminal peptide from type I interferon protects the retina in a mouse model of autoimmune uveitis. *PLoS One.* 2020;15:e0227524.
18. Ridley RB, Young BM, Lee J, et al. AAV Mediated delivery of myxoma virus M013 gene protects the retina against autoimmune uveitis. *J Clin Med.* 2019;8:2082.
19. Seeley JJ, Ghosh S. Molecular mechanisms of innate memory and tolerance to LPS. *J Leukoc Biol.* 2017;101:107–119.
20. Zielen S, Trischler J, Schubert R. Lipopolysaccharide challenge: immunological effects and safety in humans. *Expert Rev Clin Immunol.* 2015;11:409–418.
21. Chen C, Guo D, Lu G. Wogonin protects human retinal pigment epithelium cells from LPS-induced barrier dysfunction and inflammatory responses by regulating the TLR4/NF- κ B signaling pathway. *Mol Med Rep.* 2017;15:2289–2295.
22. Fields MA, Del Priore LV, Adelman RA, Rizzolo LJ. Interactions of the choroid, Bruch's membrane, retinal pigment epithelium, and neurosensory retina collaborate to form the outer blood-retinal-barrier. *Prog Retin Eye Res.* 2019;76:100803.
23. Dunn KC, Aotaki-Keen AE, Putkey FR, Hjelmeland LM. ARPE-19, a human retinal pigment epithelial cell line with differentiated properties. *Exp Eye Res.* 1996;62:155–169.
24. Deczkowska A, Keren-Shaul H, Weiner A, Colonna M, Schwartz M, Amit I. Disease-associated microglia: a universal immune sensor of neurodegeneration. *Cell.* 2018;173:1073–1081.
25. Smith JR, Hart PH, Williams KA. Basic pathogenic mechanisms operating in experimental models of acute anterior uveitis. *Immunol Cell Biol.* 1998;76:497–512.
26. Chu CJ, Gardner PJ, Copland DA, et al. Multimodal analysis of ocular inflammation using the endotoxin-induced uveitis mouse model. *Dis Model Mech.* 2016;9:473–481.
27. Guimarães MR, Leite FR, Spolidorio LC, Kirkwood KL, Rossa C. Curcumin abrogates LPS-induced pro-inflammatory cytokines in RAW 264.7 macrophages. Evidence for novel mechanisms involving SOCS-1, -3 and p38 MAPK. *Arch Oral Biol.* 2013;58:1309–1317.
28. Porro C, Cianciulli A, Trotta T, Lofrumento DD, Panaro MA. Curcumin regulates anti-inflammatory responses by JAK/STAT/SOCS signaling pathway in BV-2 microglial cells. *Biology (Basel).* 2019;8:51.
29. Fletcher TC, DiGiandomenico A, Hawiger J. Extended anti-inflammatory action of a degradation-resistant mutant of cell-penetrating suppressor of cytokine signaling 3. *J Biol Chem.* 2010;285:18727–18736.
30. Inoue M, Shinohara ML. NLRP3 inflammasome and MS/EAE. *Autoimmune Dis.* 2013;2013:859145.
31. Hernández C, Bogdanov P, Gómez-Guerrero C, et al. SOCS1-derived peptide administered by eye drops prevents retinal neuroinflammation and vascular leakage in experimental diabetes. *Int J Mol Sci.* 2019;20:3615.

32. He C, Yu CR, Mattapallil MJ, Sun L, Larkin Iii J, Egwuagu CE. SOCS1 mimetic peptide suppresses chronic intraocular inflammatory disease (uveitis). *Mediators Inflamm.* 2016;2016: 2939370.
33. Gao W, Zhao Z, Yu G, et al. VEGI attenuates the inflammatory injury and disruption of blood-brain barrier partly by suppressing the TLR4/NF-kappaB signaling pathway in experimental traumatic brain injury. *Brain Res.* 2015;1622:230–239.
34. Vigneswara V, Esmaili M, Deer L, Berry M, Logan A, Ahmed Z. Eye drop delivery of pigment epithelium-derived factor-34 promotes retinal ganglion cell neuroprotection and axon regeneration. *Mol Cell Neurosci.* 2015;68:212–221.
35. Zhang X, Li Y, Cheng Y, et al. Tat PTD-endostatin: a novel anti-angiogenesis protein with ocular barrier permeability via eye-drops. *Biochim Biophys Acta.* 2015;1850:1140–1149.